Journal of Experimental Botany, Vol. 67, No. 10 pp. 3109–3121, 2016
doi:10.1093/jxb/erv555 Advance Access publication 8 February 2016
This paper is available online free of all access charges (see http://jxb.oxfordjournals.org/open_access.html for further details)

RESEARCH PAPER

Carbon isotope discrimination as a diagnostic tool for C_4 photosynthesis in C_3-C_4 intermediate species

Hugo Alonso-Cantabrana* **and Susanne von Caemmerer**

Division of Plant Sciences, Research School of Biology, The Australian National University, Canberra, ACT 0200, Australia

* To whom correspondence should be addressed. E-mail: hugo.alonso@anu.edu.au

Received 22 October 2015; Revised 9 December 2015; Accepted 11 December 2015

Editor: Christine Raines, University of Essex

Abstract

The presence and activity of the C_4 cycle in C_3-C_4 intermediate species have proven difficult to analyze, especially when such activity is low. This study proposes a strategy to detect C_4 activity and estimate its contribution to overall photosynthesis in intermediate plants, by using tunable diode laser absorption spectroscopy (TDLAS) coupled to gas exchange systems to simultaneously measure the CO_2 responses of CO_2 assimilation (*A*) and carbon isotope discrimination (*Δ*) under low O_2 partial pressure. Mathematical models of C_3-C_4 photosynthesis and *Δ* are then fitted concurrently to both responses using the same set of constants. This strategy was applied to the intermediate species *Flaveria floridana* and *F. brownii*, and to *F. pringlei* and *F. bidentis* as C_3 and C_4 controls, respectively. Our results support the presence of a functional C_4 cycle in *F. floridana*, that can fix 12–21% of carbon. In *F. brownii*, 75–100% of carbon is fixed via the C_4 cycle, and the contribution of mesophyll Rubisco to overall carbon assimilation increases with CO_2 partial pressure in both intermediate plants. Combined gas exchange and *Δ* measurement and modeling is a powerful diagnostic tool for C_4 photosynthesis.

Key words: Carbon isotope discrimination, C_3-C_4, intermediate photosynthesis, *Flaveria*, *F. brownii*, *F. floridana*.

Introduction

C_4 photosynthesis is a highly efficient carbon fixation system characterized by the presence of a biochemical carbon pump with the capacity of increasing the CO_2 partial pressure (pCO_2) at the site of ribulose 1,5-bisphosphate carboxylase/oxygenase (Rubisco) to concentrations higher than ambient air (Hatch *et al.*, 1967; Hatch, 1987; Ehleringer *et al.*, 1991). This increases photosynthetic rates and reduces photorespiration, potentially improving nitrogen and water use efficiency (Hibberd *et al.*, 2008; Langdale, 2011). Most C_4 species show a common anatomical pattern, called Kranz anatomy, that leads to the separation of enzyme functions in two compartments, the mesophyll and the bundle sheath cell (Brown, 1975). CO_2 is first hydrated into bicarbonate in the mesophyll cell cytoplasm in a reversible reaction catalyzed by carbonic anhydrase (CA) (Badger and Price, 1994). Carbon is then fixed by phosphoenol pyruvate carboxylase (PEPC), localized exclusively in the mesophyll, into four-carbon acids that diffuse to the internally adjacent bundle sheath cell, where they are decarboxylated and the released CO_2 is refixed by Rubisco.

The most productive crops, such as maize, sorghum and sugar cane, are C_4 plants, exemplifying the higher efficiency of this system over the C_3 photosynthetic pathway present in most plant species, including major crops like wheat and rice. For this reason, there is currently a strong interest in implementing the advantages of C_4 photosynthesis in to C_3

© The Author 2016. Published by Oxford University Press on behalf of the Society for Experimental Biology.
This is an Open Access article distributed under the terms of the Creative Commons Attribution License (http://creativecommons.org/licenses/by/3.0/), which permits unrestricted reuse, distribution, and reproduction in any medium, provided the original work is properly cited.

Downloaded from http://jxb.oxfordjournals.org/ at Australian National University on January 10, 2017

crops with the aim of increasing yield, to keep pace with the food needs of a growing world population (von Caemmerer *et al.*, 2012; Karki *et al.*, 2013; Leegood, 2013). This kind of approach is boosting research on genetic, biochemical and physiological aspects of C_4 photosynthesis. However, the initial phases of these initiatives are not expected to produce fully functional C_4 plants, but plants showing incomplete C_4 phenotypes like those observed in C_3-C_4 intermediate species, which have been considered remnants of the evolution from C_3 ancestors to C_4 plants (Rawsthorne, 1992; Sage *et al.*, 2011). They show Kranz or Kranz-like leaf anatomy, but the activity of C_4-related enzymes, such as PEPC, is lower compared to strict C_4 plants, and enzyme compartmentation is incomplete, with Rubisco and PEPC present in both the mesophyll and the bundle sheath cells (Cheng *et al.*, 1988; Brown and Hattersley, 1989; Byrd *et al.*, 1992). These factors reduce the efficiency of the carbon concentrating mechanism. In intermediate plants, a photorespiratory CO_2 pump, also known as the C_2 cycle or glycine shuttle, transports glycine formed during mesophyll photorespiration to the bundle sheath where it is decarboxylated and the CO_2 refixed, thus increasing overall CO_2 assimilation rate and reducing the effect of photorespiration (Monson *et al.*, 1984; Sage *et al.*, 2012; Schulze *et al.*, 2013; Keerberg *et al.*, 2014). The genus *Flaveria* has been the focus of numerous studies in the past because it comprises C_3, C_4 and C_3-C_4 intermediate species, the later showing different degrees of C_4 activity (Ku *et al.*, 1983; McKown *et al.*, 2005).

The C_4 cycle contribution to growth has been difficult to quantify in intermediate species. In these plants, a steeper initial slope in the CO_2 response of the CO_2 assimilation rate compared to a strict C_3 plantis expected. However, this trait is also affected by Rubisco content and its kinetic properties, so conclusions are not straightforward (von Caemmerer, 2000; von Caemmerer and Quick, 2000). Another important manifestation of C_4 activity in intermediate species is a reduction of the O_2 sensitivity of CO_2 assimilation and the compensation point (Γ) due to a proportion of Rubisco being contained in the bundle sheath (BS) and thus not in direct contact with air (Byrd and Brown, 1989; Dai *et al.*, 1996). With the photorespiratory pump causing a similar effect, separating and quantifying the contribution of each biochemical pathway through this approach is not possible. The C_4 cycle activity relative to overall photosynthesis in intermediates has been estimated in the past by metabolite profiling, but recent reports indicate that metabolite accumulation is strongly dependent on the leaf zone sampled and its developmental stage (Monson *et al.*, 1986; Leegood and von Caemmerer, 1994; Wang *et al.*, 2014).

In order to develop a deeper understanding of the physiology of both natural and artificial C_3-C_4 intermediates, better tools are needed to evaluate the contribution of C_4 photosynthesis to overall assimilation. One signature of the activity of PEPC as the initial CO_2 fixation enzyme is a change in carbon isotopic discrimination (Δ) during photosynthesis. Whereas Rubisco has a strong preference for the lighter isotope, ^{12}C, over the heavier isotope, ^{13}C, PEPC is less discriminating, which causes an important difference in the biochemical fractionation between C_3 and C_4 plants (O'Leary, 1981; Farquhar, 1983). Incomplete C_4 photosynthesis in C_3-C_4 intermediates is also reflected in Δ, with both PEPC and mesophyll Rubisco acting as the initial CO_2 fixing enzymes and their relative activities determining the resulting Δ. Mathematical models describing CO_2 assimilation and isotopic discrimination in these plants have been previously developed (von Caemmerer and Hubick, 1989; von Caemmerer, 1992). However, attempts to characterize *Flaveria* intermediate species by studying carbon-isotope ratios in dry matter resulted in C_3-like profiles, and were interpreted as having little or no contribution of the C_4 system to plant growth, which was in contradiction to results from metabolite analysis (Monson *et al.*, 1988; Byrd *et al.*, 1992).

Tunable diode laser (TDL) absorption spectroscopy allows relatively rapid measurements of Δ concurrently with gas exchange, and has been used to analyze and compare C_3 and C_4 species (Tazoe *et al.*, 2011; von Caemmerer *et al.*, 2014). The present work uses this technique, combined with mathematical modeling, as a tool to determine the presence and contribution of C_4 photosynthesis in C_3-C_4 intermediate plants. An updated mathematical model of carbon isotope discrimination for C_3-C_4 intermediate species is proposed, which considers the effect of mesophyll conductance and allows the calculation of the biochemical fractionation. The strategy was applied to the study of *Flaveria bidentis* (C_4), *F. pringlei* (C_3), *F. floridana* (C_3-C_4) and *F. brownii* (C_4-like). *F. floridana* has been described as a C_2 plant with elevated PEPC activity, but it was unclear if a C_4 cycle is actually contributing to total carbon assimilation in this species (Monson *et al.*, 1986, 1988; Leegood and von Caemmerer, 1994; Dai *et al.*, 1996). *F. brownii*, on the other hand, was initially considered a C_4 species, but later experiments proved incomplete enzyme compartmentation, with a small proportion of Rubisco activity present in the mesophyll cells, and it was then reclassified as a C_4-like intermediate species (Holaday *et al.*, 1984; Monson *et al.*, 1987; Moore *et al.*, 1989). In the present study, concurrent Δ and gas exchange measurement and modeling allowed the detection and estimation of the C_4 cycle in the intermediate species, proving itself as a powerful diagnostic tool for C_4 photosynthesis.

Materials and methods

Plant material and growth conditions

Flaveria bidentis was propagated from seeds and *F. pringlei*, *F. brownii* and *F. floridana* were propagated from cuttings (Brown and Hattersley, 1989; Whitney *et al.*, 2011). Plants were grown in 30 l pots in a garden soil mix fertilized with Osmocote (Scotts, Australia) in a glasshouse under natural light conditions, at 28/18°C day/night temperatures, respectively. Pots were watered daily.

Responses of CO_2 assimilation rate and CO_2 compensation point to O_2 partial pressure

Two Li-Cor 6400XTs (Li-Cor, USA) were used to measure CO_2 assimilation at a range of reference pCO_2 (388, 0, 24, 48, 73, 97, 145, 194, 291, 388, 485, 582 and 776 μbar). N_2 and O_2 were mixed in different ratios by mass flow controllers (Omega Engineering Inc., USA) to generate a range of O_2 partial pressures (pO_2; 20, 50, 100,

Downloaded from http://jxb.oxfordjournals.org/ at Australian National University on January 10, 2017

200 and 300 mbar) supplied to the LI-6400s. Response curves of CO_2 assimilation rate (A) to intercellular pCO_2 (C_i), A/C_i curves, were repeated sequentially at each pO_2. The measurements were made at 25°C, a flow rate of 500 µmol s^{-1} and 1500 µmol quanta m^{-2} s^{-1}, inside a growth cabinet at 25°C. Four plants from each species were analyzed. The compensation point (Γ) was calculated from the A/C_i curves at each pO_2, as the intercellular CO_2 concentration where net CO_2 assimilation is zero.

To study the inhibitory effect of O_2 on assimilation rate, we compared the CO_2 assimilation rate at a reference pCO_2 of 380 µbar at each pO_2.

Concurrent gas exchange and Δ measurements and calculations of mesophyll conductance

Two Li-Cor 6400XTs (Li-Cor, USA) coupled to a tunable-diode laser absorption spectroscope (TDLAS, model TGA100A, Campbell Scientific, Inc., USA) as described in Tazoe *et al.* (2011) were used for concurrent measurements of gas exchange and carbon isotope discrimination (Bowling *et al.*, 2003; Griffis *et al.*, 2004; Pengelly *et al.*, 2012; Evans and von Caemmerer, 2013). Plants were transferred from the glasshouse to a growth cabinet with fluorescence lights (TRIL1175, Thermoline Scientific Equipment, Australia) at 25°C and one young fully expanded leaf was placed in each of the 6 cm^2 leaf chambers. Measurements were made at a leaf temperature of 25°C, a flow rate of 200 µmol s^{-1}, 1500 µmol quanta m^{-2} s^{-1} and 20 mbar pO_2. The desired pO_2 was achieved as described above and supplied to the Li-Cors 6400. Reference pCO_2 was changed stepwise to 392, 980, 686, 490, 294, 196, 98, 49 and 392 µbar and measurements were made every 4 min for at least 30 min at each pCO_2. Dark respiration (R_d) was measured at the end of an A/C_i curve at 392 µbar pCO_2 and 20 mbar pO_2 by switching off the Li-Cor lamp. Three or four plants from each species were analyzed. Δ was calculated as previously described (Evans *et al.*, 1986; Evans and von Caemmerer, 2013).

Mesophyll conductance (g_m) was calculated for *F. pringlei* from concurrent gas exchange and Δ measurements at the above range of reference pCO_2 and 19 mbar pO_2, applying the equations previously described and including the ternary effects of transpiration rate (Farquhar and Cernusak, 2012; Evans and von Caemmerer, 2013). This method is only valid for C_3 species. For intermediate and C_4 species, we assumed the same CO_2 response of g_m found in *F. pringlei*, and scaled the absolute value at ambient pCO_2 to obtain the best fit of the A and Δ models for the observed results (see Results section).

Mathematical models

The overall rate of net CO_2 assimilation (A) for C_3-C_4 intermediate plants was previously described (von Caemmerer, 1992, 2013):

$$A = A_s + A_m \tag{1}$$

where A_m is the assimilation in the mesophyll and A_s is the assimilation in the bundle sheath, which are defined as:

$$A_s = V_p + \beta F_m - L \tag{2}$$

$$A_m = V_m - R_m - (1-\beta)F_m \tag{3}$$

so:

$$A = V_m - R_m - F_m + V_p - L \tag{4}$$

where V_p is PEPC carboxylation and β is the fraction of the CO_2 produced from photorespiration in the mesophyll (F_m) that is released in the bundle sheath. For simplification, bundle sheath respiration and photorespiration are not taken into account in eq. 4. The term L is the leak rate of CO_2 out of the bundle sheath, and can be expressed as:

$$L = \phi(V_p + \beta F_m) \tag{5}$$

and

$$A = V_m - R_m - F_m + V_p - \phi(V_p + \beta F_m) \tag{6}$$

where ϕ (leakiness) is the ratio of the leak rate of CO_2 out of the bundle sheath and the supply rate of CO_2 to the bundle sheath $(V_p + \beta F_m)$. When pO_2 is low, F_m can be considered 0.

V_m and R_m are Rubisco carboxylation and day respiration in the mesophyll, respectively. V_p and V_m are calculated as described in von Caemmerer (2000):

$$V_m = \frac{C_m \cdot V_{m,max}}{C_m + K_c(1 + \frac{O}{K_o})} \tag{7}$$

$$V_p = \frac{C_m \cdot V_{p,max}}{C_m + K_p} \tag{8}$$

and

$$C_m = C_i - \frac{A}{g_m} \tag{9}$$

where C_m and C_i are mesophyll and intercellular pCO_2, respectively. K_c and K_o are the Michaelis-Menten constants for CO_2 and O_2 respectively, expressed as a partial pressure. Although the pCO_2 in the cytosol (site of PEPC carboxylation) and the chloroplast (site of Rubisco carboxylation) of the mesophyll cell are presumably different due to diffusional limitations, the same value (C_m) was assumed in both compartments (von Caemmerer, 2000, 2013; Tholen and Zhu, 2011).

When the rate of PEP regeneration is limiting, $V_p = V_{pr}$, where V_{pr} is a constant. $V_{m,max}$ is the maximum Rubisco carboxylation in the mesophyll, and $V_{p,max}$ is the maximum PEPC carboxylation (Table 1). When RuBP becomes limiting, V_m in eq. 6 can be given by an electron transport limited rate (W_j), as previously described (von Caemmerer, 2000, 2013).

Theory developed by Farquhar *et al.* (1982) and Farquhar (1983) showed that photosynthetic carbon isotope discrimination can be described by equations having diffusion and biochemistry dependent terms. The equation of Δ presented by (Griffiths *et al.*, 2007), which takes into account the effect of g_m, was modified to incorporate the ternary effects of transpiration rate as suggested by Farquhar and Cernusak (2012):

$$\Delta = \frac{1}{1-t}a' + \frac{1+t}{1-t}(a_l + b_s - \Delta_{bio})\frac{A}{g_m \cdot C_a} + \frac{1}{1-t}[(1+t)\Delta_{bio} - a']\frac{C_i}{C_a} \tag{10}$$

where a_l is the fractionations during diffusion in water and b_s is the fractionation as CO_2 enters solution. The term $t = \frac{(1+a')E}{2g^t_{ac}}$, where E denotes the transpiration rate and g^t_{ac} the total conductance to CO_2 diffusion including boundary layer and stomatal conductance. The symbol a' denotes the combined fractionation during diffusion in the boundary layer and in air, and is calculated as:

$$a' = \frac{a_b(C_a - C_l) + a(C_l - C_i)}{(C_a - C_i)} \tag{11}$$

where a is the fractionation during diffusion in air, a_b is the fractionation during diffusion in the boundary layer, and C_a, C_l, C_i are the pCO_2 in the air, leaf surface and intercellular space respectively.

Downloaded from http://jxb.oxfordjournals.org/ at Australian National University on January 10, 2017

Table 1. *Values assigned to variables for model fitting purposes*

When fitting *F. brownii* as a strict C_4 and *F. floridana* as a strict C_3 species, values were assigned to obtain the best fitting without considering measured enzyme activities.

Variable	Definition	*F. pringlei*	*F. bidentis*	*F. brownii*	*F. brownii* (strict C_4)	*F. floridana*	*F. floridana* (strict C_3)	Origin of the value
a	Fractionation during diffusion in air (‰)	4.4	4.4	4.4	4.4	4.4	4.4	Farquhar (1983)
a_b	Fractionation during diffusion through the boundary layer (‰)	2.9	2.9	2.9	2.9	2.9	2.9	Griffiths *et al.* (2007)
abs	Leaf absorptance	0.8	0.8	0.8	0.8	0.8	0.8	von Caemmerer (2000)
a_l	Fractionation during diffusion in water (‰	0.7	0.7	0.7	0.7	0.7	0.7	Griffiths *et al.* (2007)
β	Fraction of the photorespired CO_2 released in the bundle sheath	1	1	1	1	1	1	Assigned
b_3	Fractionation during carboxylation by Rubisco (‰)	29	29	29	29	29	29	Roeske and O'Leary (1984)
b_4	Combined fractionation by the C_4 cycle (‰)	na	−5.7	−5.7	−5.7	−5.7	na	O'Leary (1981)
b_s	Fractionation during CO_2 dissolution in water (‰	1.1	1.1	1.1	1.1	1.1	1.1	von Caemmerer (1992)
c	g_m scaling constant	0.666[a]	0.8[b]	0.666[b]	0.666[b]	0.78[b]	0.78[b]	[a], measured in this work; [b], assigned from model fitting
e	fractionation during mitochondrial respiration	2.91	3.54	3.51	3.51	3.72	3.72	Calculated as $e=\delta^{13}C_{cylinder}-\delta^{13}C_{atmosphere}$
F	Correction coefficient for spectral quality	0.15	0.15	0.15	0.15	0.15	0.15	von Caemmerer (2000)
J_t	Total electron transport rate (μmol electrons m^{-2} s^{-1})	120	400	440	700	250	0	Assigned [von Caemmerer (2000), eq. 5.17]
J_m	Electron transport rate allocated to mesophyll C_3 cycle	120	0	40	0	200	240	Assigned [von Caemmerer (2000), eq. 5.17]
K_C	Rubisco Michaelis–Menten constant for CO_2 (μbar)	359	605	383	383	395	395	Kubien *et al.* (2008)
K_O	Rubisco Michaelis–Menten constant for O_2 (μbar)	528 000	507 000	300 000	300 000	544 000	544 000	Kubien *et al.* (2008)
K_P	PEPC Michaelis–Menten constant for PEP (μbar)	n.a.	80	80	n.a.	80	n.a.	Bauwe (1986)
R_d	Mitochondrial respiration (μmol m^{-2} s^{-1})	0.6	0.4	1.3	1.3	1.7	1.7	Measured in the dark in this work
s	Fractionation during leakage (‰)	n.a.	1.8	1.8	1.8	1.8	n.a.	von Caemmerer (1992)
$V_{m, max}$	Maximum Rubisco carboxylation rate in the mesophyll (μmol m^{-2} s^{-1})	60[a]	0[b]	15[b]	0[b]	90[a]	130[b]	[a], measured in this work; [b], assigned
$V_{P, max}$	Maximum PEP carboxylation rate (μmol m^{-2} s^{-1})	0[a]	90[a]	80[a]	80[b]	15[a]	0[b]	[a], measured in this work; [b], assigned
V_{Pr}	PEP regeneration rate (μmol m^{-2} s^{-1})	0	36	32	50	8	0	Assigned
ϕ	Leakiness	n.a.	0.28	0.21	0.3	0.40	n.a.	Assigned from model fitting
θ	Empirical curvature factor	0.1	0.1	0.1	0.1	0.1	0.1	Ubierna *et al.* (2011)

n.a., not applicable.

Downloaded from http://jxb.oxfordjournals.org/ at Australian National University on January 10, 2017

The biochemical fractionation, Δ_{bio}, is the integrated net biochemical discrimination, and depends on the biochemistry of net CO_2 uptake (Griffiths *et al.*, 2007).

When Δ and g_m are known, Δ_{bio} can be solved from equation 10, resulting in:

$$\Delta_{bio} = \frac{\Delta - \frac{1}{1-t}a'\frac{C_a - C_i}{C_a} - \frac{1+t}{1-t}a_i\frac{A}{g_m \cdot C_a}}{\frac{1+t}{1-t}\left(\frac{C_i}{C_a} - \frac{A}{g_m \cdot C_a}\right)} \tag{12}$$

Because g_m was obtained from combined measurement of Δ and gas exchange in the C_3 species *F. pringlei*, Δ and g_m are not independent and we could not estimate Δ_{bio} from eq. 12. For the intermediate and C_4 species, g_m was calculated independently of the Δ measurements as described in the Materials and Methods section, so Δ_{bio} could be estimated from eq. 12 for *F. floridana*, *F. brownii* and *F. bidentis*.

For modeling purposes, or when Δ is unknown, Δ_{bio} can be derived from von Caemmerer's (1992) equation A17:

$$\frac{R_i}{R_p} = 1 + (b_3 - \frac{fF_m + eR_m}{A}) + \frac{A_s}{A}[(b_3 - s)\phi + \frac{(b_4 - b_3)V_p - f\beta F_m}{V_p + \beta F_m}] - \frac{fF_s + eR_s}{A}\phi$$

where R_i and R_p are the molar abundance ratios of $^{13}C/^{12}C$ in the intercellular space and the photosynthetic product, respectively.

$$\Delta_{bio} = \frac{R_i}{R_p} - 1$$

Thus:

$$\Delta_{bio} = (b_3 - \frac{fF_m + eR_m}{A}) + \frac{A_s}{A}[(b_3 - s)\phi + \frac{(b_4 - b_3)V_p - f\beta F_m}{V_p + \beta F_m}] - \frac{fF_s + eR_s}{A}\phi \tag{13}$$

The factor b_3 is the Rubisco fractionation, and b_4 is the combined fractionation of PEP carboxylation and the preceding isotope equilibrium during dissolution of CO_2 and conversion to bicarbonate; s is the fractionation during leakage of CO_2 out of the bundle sheath; e is the fractionation during mitochondrial respiration; f is the fractionation during photorespiration; R_m and R_s are the mitochondrial respiration rates in the mesophyll and the bundle sheath in the light, respectively. It was assumed that $R_d = R_m + R_s$, and $R_m = R_s = 0.5R_d$. The factors F_m and F_s are the photorespiration rates derived from Rubisco oxygenation in the mesophyll and the bundle sheath, respectively. When pO_2 is low, F_m and F_s are close to 0, so equation 13 simplifies to:

$$\Delta_{bio} = (b_3 - \frac{eR_m}{A}) + \frac{A_s}{A}[(b_3 - s)\phi + (b_4 - b_3)] - \frac{eR_s}{A}\phi \tag{14}$$

The parameter e needs to account for differences between the isotopic composition of CO_2 during plant growth and during the measurements, because the substrates used during respiration are most likely carbohydrates assimilated before the experiment (Wingate *et al.*, 2007). No fractionation during mitochondrial respiration was assumed in this work, so e was calculated as the difference between $\delta^{13}C$ in the CO_2 cylinder used during the experiments and $\delta^{13}C$ in the atmosphere during growth conditions ($e = \delta^{13}C_{cylinder} - \delta^{13}C_{atmosphere}$) (Tazoe *et al.*, 2009; Pengelly *et al.*, 2010). In this work, $\delta^{13}C_{cylinder}$ was between −4.12‰ and −5.14‰, and $\delta^{13}C_{atmosphere}$ was assumed to be −8‰ (Table 1).

In vitro enzyme activity assays

Leaf discs (0.5 cm^2) were collected from the leaves used for gas exchange experiments and frozen in liquid nitrogen immediately after the experiment. Soluble protein was extracted by grinding one frozen leaf disc in a cold Tenbroeck homogenizer with 0.5 ml extraction buffer [50 mM HEPES, 1 mM EDTA, 0.1% (v/v) Triton X-100, 10 mM DTT, 1% (w/v) PVPP, 1% (v/v) protease inhibitor cocktail (Sigma), pH 7.8]. Extracts were centrifuged at 13 000 rpm for 30 s. Spectrophotometric assays were performed to determine Rubisco and PEPC activities as described in Pengelly *et al.* (2010).

CA activity was measured in the same extract used for PEPC and Rubisco activity measurements, using a membrane inlet mass spectrometer to measure the rates of ^{18}O exchange from labeled $^{13}C^{18}O_2$ to $H_2{}^{16}O$ at 25°C with a subsaturating total carbon concentration of 1 mM (Badger and Price, 1989; von Caemmerer *et al.*, 2004; Cousins *et al.*, 2008). The hydration rates were calculated from the enhancement in the rate of ^{18}O loss over the uncatalyzed rate, and the nonenzymatic first-order rate constant was applied at pH 7.4 (k_c=6.22x10^{-11}/[H^+]+3.8x10^{-2}=0.0396), appropriate for the mesophyll cytosol, at a CO_2 concentration of 8 µM, which is approximately the CO_2 concentration in the mesophyll of *F. bidentis* (Jenkins *et al.*, 1989; von Caemmerer *et al.*, 2004). When CA is in the chloroplast, which is tipically the case in C_3 plants like *F. pringlei*, our calculations underestimate its *in planta* activity by ~10% due to the effect of the higher chloroplastic pH on k_c (k_c=0.0442 at pH 8).

Results

O_2 response of CO_2 assimilation rate and compensation point

The effect of pO_2 on CO_2 assimilation rate and the compensation point (Γ) was measured at 380 µbar reference CO_2, an irradiance of 1500 µmol quanta m^{-2} s^{-1} and 25 °C (Fig. 1).

In *F. pringlei*, increasing pO_2 caused a decrease in CO_2 assimilation rate, a response typical of a C_3 plant. Consistent with this, the Γ increased with increasing pO_2, ranging from 5.6 ubar at 19 mbar O_2 to 53 µbar at 285 mbar O_2.

In the C_4 species *F. bidentis*, the effect of oxygen was very small, with only a 5% decrease in CO_2 assimilation rate at the highest tested pO_2. Γ in these plants barely changed with pO_2, and ranged from 0.2 to 1.2 µbar.

The effect of O_2 on Γ in *F. brownii* was also very small and similar to the C_4 species *F. bidentis,* ranging from 1.3 to 3.1 µbar (Fig. 1b). However, the inhibitory effect of O_2 on CO_2 assimilation rate was more pronounced, and resulted in an intermediate response of CO_2 assimilation rate to increasing pO_2 (Fig. 1a).

The O_2 response of Γ in *F. floridana* was intermediate between C_3 and C_4 species (2.3–18 µbar; Fig. 1b), as has been previously shown (Ku *et al.*, 1991). However, in our experiments the inhibitory effect of O_2 on photosynthesis was smaller than that previously reported by these authors and strikingly similar to that in *F. brownii* when pO_2 was 200 mbar or lower, despite the important differences in the enzyme compartmentation between these two species (Fig. 1a). Only at 290 mbar O_2 the inhibition of photosynthesis was higher for *F. floridana*, with a reduction of a 22%, compared to that in *F. brownii* (15% inhibition).

Stomatal conductance and C_i increased slightly with pO_2, with the exception of *F. bidentis*, which remained stable, and

Downloaded from http://jxb.oxfordjournals.org/ at Australian National University on January 10, 2017

were considerably higher in the C_3 species *F. pringlei* at any pO_2 (Supplementary Fig. S1 at *JXB* online).

Rubisco, PEPC and CA activity

In vitro Rubisco, PEPC and CA activities were analyzed in extracts from the same leaves on which the concurrent gas exchange and Δ measurements were made (Fig. 2). Rubisco activity was higher in *F. floridana* (average of 74.9 μmol m^{-2} s^{-1}), followed by *F. pringlei* (60.5 μmol m^{-2} s^{-1}), *F. brownii* (49.2 μmol m^{-2} s^{-1}) and *F. bidentis* (39.7 μmol m^{-2} s^{-1}). PEPC activity was lowest in *F. pringlei* (2.9 μmol m^{-2} s^{-1}) and, notably, four times higher in *F. floridana* (13.8 μmol m^{-2} s^{-1}). *F. brownii* showed a PEPC activity closer to that of *F. bidentis* (79.3 and 91.8 μmol m^{-2} s^{-1} respectively). CA activity was similar and high in *F. bidentis* and *F. brownii* (1278.7 and 1464.5 μmol m^{-2} s^{-1} respectively), and lower in *F. pringlei* and *F. floridana* (614.9 and 623.6 μmol m^{-2} s^{-1} respectively).

The relative activity of PEPC to Rubisco was lowest in *F. pringlei* and highest in *F. bidentis* (Fig. 2b). *F. floridana* showed a PEPC:Rubisco ratio 3.4 times greater than the C_3 species, and *F. brownii* was closer to the C_4 species.

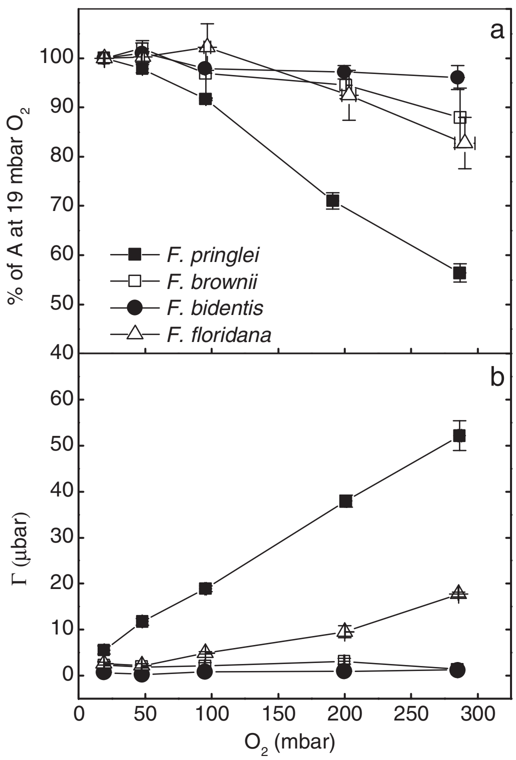

Fig. 1. The responses of (a) CO_2 assimilation rate, *A* and (b) compensation point (Γ) in *F. pringlei*, *F. floridana*, *F. brownii* and *F. bidentis* to changes in atmospheric pO_2. Assimilation rate is expressed as a percentage of the assimilation rate at 19 mbar O_2 (average of 28.7 ± 1.13 μmol m^{-2} s^{-1} for *F. pringlei*, 24.2 ± 1.52 for *F. floridana*, 20.6 ± 1.2 for *F. brownii* and 21.7 ± 0.49 for *F. bidentis*). Measurements were made at 25°C and 385 μbar CO_2 (R), and an irradiance of 1500 μmol m^{-2} s^{-1}. Values represent averages and standard error of four replicates.

CO_2 assimilation rate and carbon isotope discrimination

Measurements of carbon isotope discrimination concurrently with gas exchange were performed under a range of CO_2 concentrations at 19 mbar O_2 on 3–4 plants from each species (Fig. 3). At this low pO_2, photorespiration is greatly reduced and the effect of the C_2 cycle is negligible. Thus, small differences in the level of C_4 activity or mesophyll Rubisco activity are easier to detect.

F. pringlei and *F. bidentis* showed the typical C_3 and C_4 response of CO_2 assimilation rate to increasing C_i, respectively (Fig. 3a). The initial slope of the A/C_i curve in *F. floridana* was closer to that in the C_3 species, *F. pringlei*, whereas that of *F. brownii* was more similar to that of the C_4 species, *F. bidentis*, although in both intermediate species the sharp saturation typical of the C_4 species was missing. The maximum apparent assimilation rates in both intermediates were higher than those of the C_3 and C_4 species.

Carbon isotope discrimination measured over the defined range of pCO_2 provided clear differences between the four species (Fig. 3b). Δ was greatest in *F. pringlei* at any C_i, ranging from 16‰ to 24.4‰. Discrimination in *F. floridana* followed a similar trend than that in the C_3 species, with Δ generally increasing with C_i, but Δ was lower than in *F. pringlei* across the whole experimental range, ranging from 12.2‰ to 18.6‰. The response of C_i/C_a to CO_2 concentration was parallel to that of Δ in *F. pringlei* and *F. floridana*, reflecting the strong dependence of Δ on the ratio C_i/C_a in C_3 species and also in

Downloaded from http://jxb.oxfordjournals.org/ at Australian National University on January 10, 2017

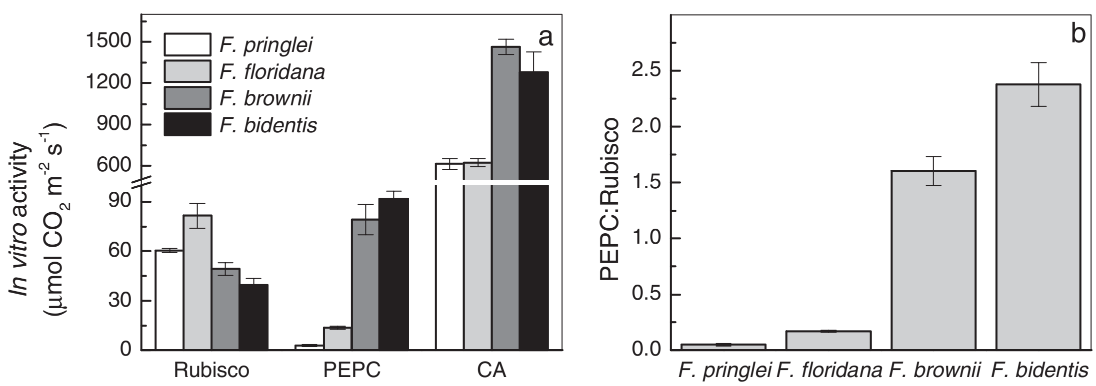

Fig. 2. (a) *In vitro* Rubisco, PEPC and CA activities in *F. pringlei*, *F. floridana*, *F. brownii* and *F. bidentis*, measured from samples of the same leaves used for gas exchange and expressed on a leaf area basis. (b) PEPC to Rubisco activity ratio in these experiments. Values represent mean and standard error of four experimental replicates.

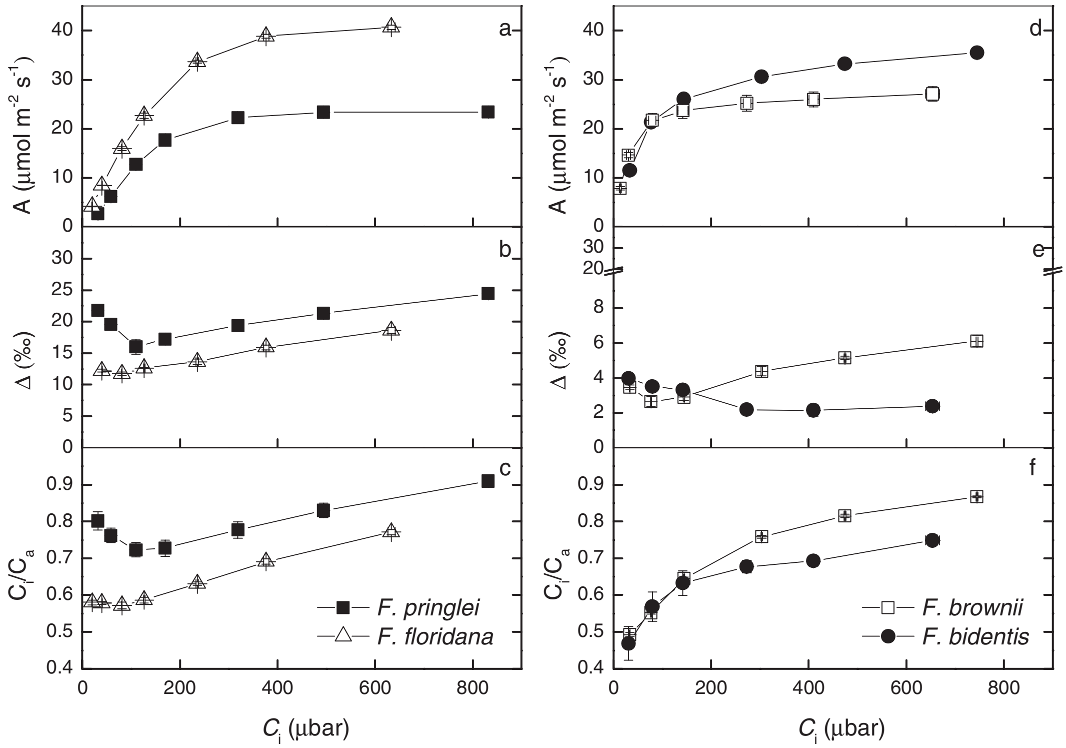

Fig. 3. Concurrent measurements of (a, d) CO_2 assimilation rate, *A*, (b, e) carbon isotope discrimination, *Δ*, and (c, f) the ratio of intercellular to ambient CO_2, C_i/C_a, as a function of intercellular CO_2 (C_i) in *F. pringlei*, *F. floridana*, *F. brownii* and *F. bidentis*. Values represent averages and standard error of 4 replicates. Measurements were made at 19 mbar O_2, a leaf temperature of 25°C and an irradiance of 1500 µmol $m^{-2}s^{-1}$.

F. floridana (Fig. 3c). The initial decrease of *Δ* in *F. pringlei* is also caused by a drop in C_i/C_a, which is in turn driven by a reduction of stomatal conductance with increasing C_i when C_i is lower than 200µbar.

In *F. bidentis*, as expected from a C_4 plant, discrimination was low (2–4‰) and decreased slightly with increasing C_i. *Δ* in *F. brownii* was similar to *F. bidentis* at C_i under 95 µbar (3.5–2.6‰), but above that the value of *Δ* increased with increasing C_i, to a maximum of 6.1‰.

Measured *Δ* is shown with respect to C_i/C_a in Fig. 4. The theoretical lines assume infinite mesophyll conductance, which explains why both *F. pringlei* and *F. floridana* fell below the theoretical response for C_3 plants, with *Δ* and C_i/C_a generally lower in *F. floridana*. In *F. bidentis*, the result was as predicted by a theoretical CO_2 response of *Δ* for a C_4 plant when $\phi = 0.25$, whereas *F. brownii* only fitted the expected response at low C_i/C_a, with *Δ* higher than predicted at high C_i/C_a.

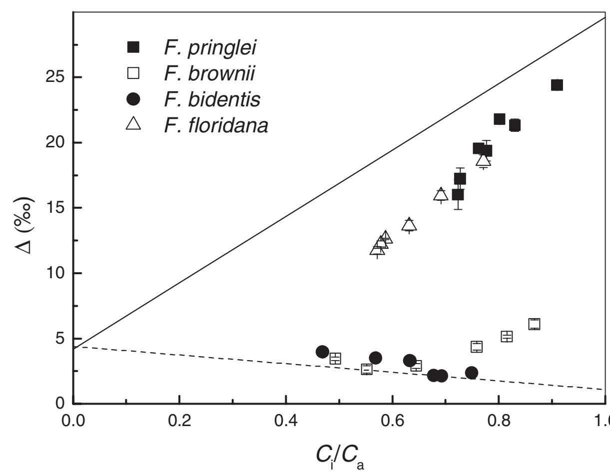

Fig. 4. Observed carbon isotope discrimination, *Δ* expressed as a function of the ratio of intercellular to ambient CO_2, C_i/C_a, in *F. pringlei*, *F. floridana*, *F. brownii* and *F. bidentis*. Values are the same as plotted in Fig. 3. Solid line represents the theoretical response of *Δ* to C_i/C_a in C_3 plants ($\Delta = 4.4 + \frac{C_i}{C_a}(29 - 4.4)$; (Roeske and O'Leary, 1984; Evans *et al.*, 1994). Dashed line represents the theoretical response of *Δ* to C_i/C_a in C_4 plants, $\Delta = 4.4 + \frac{C_i}{C_a}[-5.7 - 4.4 + \phi(29 - 1.8)]$ (Henderson *et al.*, 1992) when ϕ=0.25.

Modeling CO_2 assimilation rate and carbon isotope discrimination in C_3-C_4 intermediate species

In order to evaluate the contribution of the C_4 cycle to overall photosynthesis in the intermediate species *F. floridana* and *F. brownii*, the mathematical models proposed here for *A* and *Δ* responses to C_i (eqs 6 and 10, respectively) were fitted concurrently to the observed results (Fig. 5). By simultaneously fitting both models using the same set of parameters, the accuracy of the predictions increases because some combinations of assigned constants that may result in a good fit for one of the models are unacceptable for the other. For comparison, the same strategy was also applied to the C_3 and C_4 species (see Supplementary Fig. S2).

Table 1 shows the values assigned for fitting purposes and their source. Rubisco K_C and K_O (Michaelis–Menten constants for CO_2 and O_2, respectively) in the four *Flaveria*

Downloaded from http://jxb.oxfordjournals.org/ at Australian National University on January 10, 2017

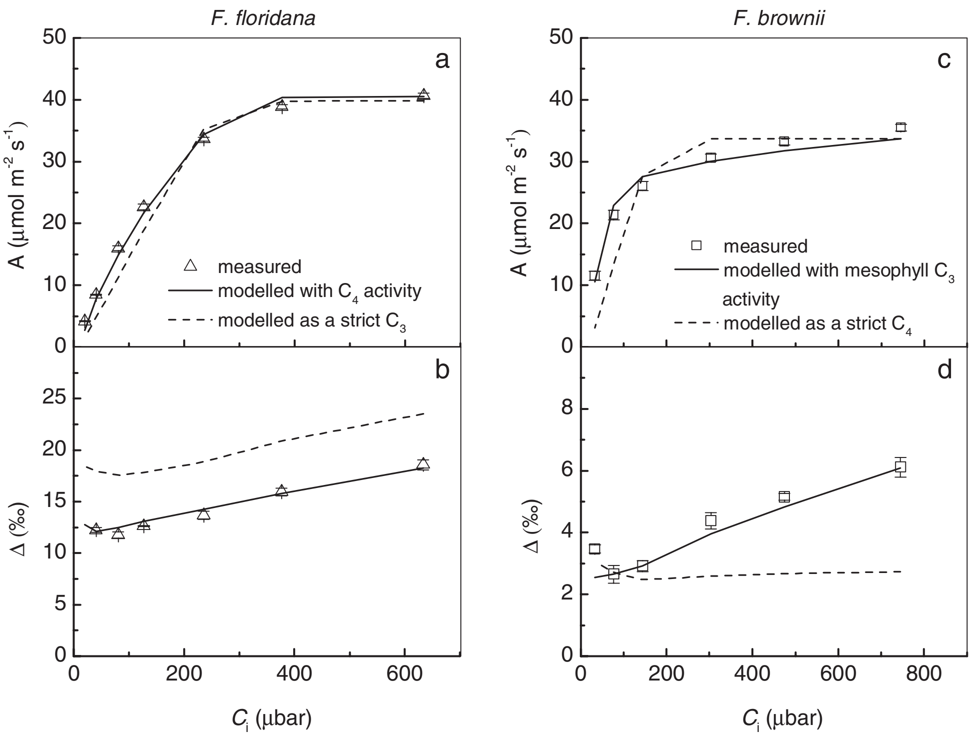

Fig. 5. Comparison between modeled and measured responses of CO_2 assimilation rate, *A*, and carbon isotope discrimination, *Δ*, to variation in intercellular pCO_2, C_i, in the C_3-C_4 intermediate species *F. floridana* and *F. brownii*. Measured *A* (a) and *Δ* (b) as a function of C_i in *F. floridana* (empty triangles), compared with the modeled responses predicted by C_3-C_4 photosynthetic model assuming an active C_4 cycle (solid lines) or no C_4 cycle activity (dashed lines). Measured *A* (c) and *Δ* (d) as a function of C_i in *F. brownii* (white squares), compared with the modelled responses using the C_3-C_4 models assuming Rubisco activity in the mesophyll cells (solid lines) or a strict compartmentalization of Rubisco in the bundle sheath cells (dashed lines). Parameters used for model simulations are presented in Table 1.

species analyzed here have been previously reported (Kubien *et al.*, 2008), and $V_{c,max}$ and $V_{p,max}$ are from our own *in vitro* experiments. We assigned reasonable values for maximum electron transport (J_{max}). Leakiness (ϕ) was assigned so that the sum of the squares of the variances between the measured and modeled *A*, and between the measured and modeled *Δ*, was minimum. The distribution of Rubisco between the mesophyll and the bundle sheath in the intermediate species can be adjusted in the models by the assigned $V_{m,max}$ (maximum rate of Rubisco carboxylation in the mesophyll) value. When $V_{m,max}$ equals the $V_{c,max}$ observed *in vitro*, all Rubisco is in the mesophyll. A lower asigned $V_{m,max}$ indicates that part of the Rubisco activity is contained in the bundle sheath cells.

Mesophyll conductance (g_m) for *F. pringlei* was calculated from concurrent gas exchange and carbon isotope discrimination measurements at 19 mbar O_2 and a range of reference pCO_2 as previously described (Tazoe *et al.*, 2011; Farquhar and Cernusak, 2012; Evans and von Caemmerer, 2013). Results show that g_m decreases from 0.62 ± 0.1 to 0.33 ± 0.03 mol m^{-2} s^{-1} bar^{-1} with increasing C_i when atmospheric pCO_2 is lower than ambient, and then remains stable at higher pCO_2 (Fig. 6). The CO_2 dependence of g_m in *F. pringlei* is described by the polinomial function $g_m=10^{-6}\cdot C_i^2-0.0013\cdot C_i+c$, where c=0.666. In C_4 and C_3-C_4 intermediate species, g_m cannot be obtained from concurrent gas exchange and $\Delta^{13}C$ measurements, so the same CO_2 dependence of g_m was assumed for *F. bidentis*, *F. brownii* and *F. floridana*, and the constant *c* was calculated from model fitting so that the sum of variances between the measured and modeled *A*, and between the measured and modeled *Δ*, was minimum (Table 1). The resulting g_m are shown in Fig. 6. Methods for obtaining g_m in C_4 and C_3-C_4 intermediate species, based on ^{18}O discrimination measurements, are currently being developed (S. von Caemmerer, unpublished results).

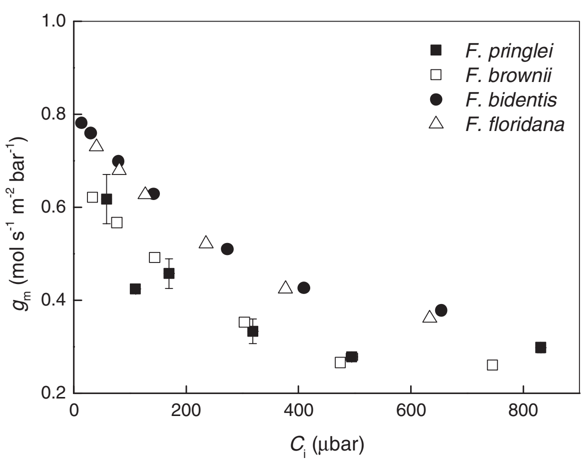

Fig. 6. Response of mesophyll conductance (g_m) to changes in atmospheric pCO_2. In *F. pringlei*, g_m was calculated from concurrent gas exchange and *Δ* measurements made at 19 mbar pO_2. The values for *F. floridana*, *F. brownii* and *F. bidentis* were assigned assuming the same response of g_m to C_i as observed in *F. pringlei*, scaled from model fitting.

The *A* and *Δ* responses to increasing C_i predicted with this strategy were reasonably close to the measured values for *F. pringlei* and *F. bidentis* (Supplementary Fig. S2).

Downloaded from http://jxb.oxfordjournals.org/ at Australian National University on January 10, 2017

In an exercise to prove the predictive value of these models for the presence of low levels of activity of the C_4 component, we attempted to fit the models for *F. floridana* under two different premises. In one case, we assumed a certain level of effective C_4 cycle contribution to overall carbon assimilation (Fig. 5a, b, solid lines). In the second case, we considered no C_4 activity and values were assigned to obtain the best possible fitting ignoring the measured enzyme activities (Fig. 5a, b, dashed lines). The models could only be fitted to the measured values of Δ and A if some C_4 activity, specified by a $V_{p,max}$ close to our *in vitro* measurements, was assumed.

A similar approach was used with *F. brownii*. In one case, the models were fitted assuming the presence of Rubisco in the mesophyll, and in the other case the model was fitted as if it were a strict C_4 plant (Fig. 5c, d). The predicted responses approached the measured values only if ~30% of Rubisco activity was located in the mesophyll ($V_{m,max}$ =15 μmol m^{-2} s^{-1}; observed *in vitro* $V_{c,max}$ =50 μmol m^{-2} s^{-1}).

A comparison of Δ and Δ_{bio} highlights the fact that CO_2 diffusion processes have a large influence on Δ (Figs 3, 7). Δ_{bio} was calculated from eq. 12 using gas exchange and Δ measured values. Calculation of Δ_{bio} factors out the contribution from CO_2 diffusion and shows that the biochemical fractionations are different in the species analyzed. In *F. floridana*, Δ_{bio} was high and increasing with C_i. In *F. brownii*, Δ_{bio} also increased with increasing C_i, whereas in the C_4 species *F. bidentis* Δ_{bio} generally decreases with C_i.

The A and Δ responses to C_i could be modeled assuming a constant g_m without important differences (data not shown). However, the calculation of biochemical fractionation (Δ_{bio}) from eq. 12 is dependent on g_m, and thus the dependence of g_m on C_i must have an effect on Δ_{bio}. To show the magnitude of this effect, the C_i response of Δ_{bio} was calculated from eq. 12 and the gas exchange and Δ measurements, assuming either variable g_m, assigned as previously explained in this section, or constant g_m, calculated as the average of the variable g_m values obtained for each species (see Supplementary Fig. S3). As a reference, the C_i response of Δ_{bio} was calculated from eq. 14 (modelled Δ_{bio}) after fitting the models for the C_i responses of A and Δ using variable g_m.

Estimation of the C_4 (bundle sheath) photosynthesis contribution to total photosynthesis

The relative contribution of the bundle sheath to total photosynthesis in the intermediate species was estimated from A_s in eq. 2, after fitting the models to our observed results (Fig. 8). Because the experiments were performed under low O_2, photorespiration is greatly reduced and it can be assumed that all the CO_2 assimilated in the bundle sheath is transported by the C_4 cycle. The contribution of the bundle sheath to total photosynthesis in both *F. floridana* and *F. brownii* decreased with increasing C_i. In *F. brownii*, almost all carbon was fixed by Rubisco in the bundle sheath at very low C_i, but up to 25% of fixation occurred via Rubisco in the mesophyll at high C_i. In *F. floridana*, the maximum estimated contribution of the bundle sheath photosynthesis via the C_4 cycle was 21% at very low C_i and it dropped to 12% at the highest C_i analyzed.

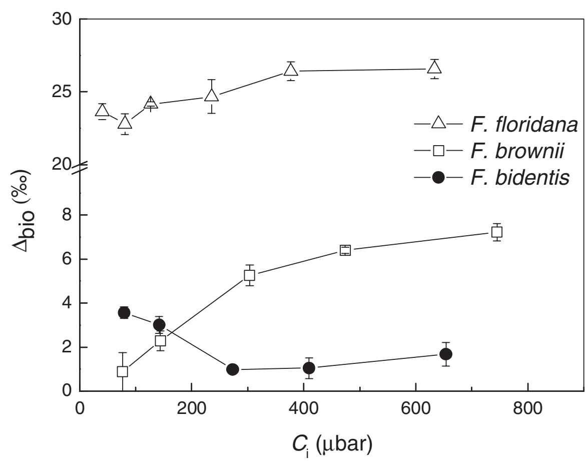

Fig. 7. Biochemical fractionation (Δ_{bio}), as a function of intercellular CO_2 (C_i) in *F. floridana*, *F. brownii* and *F. bidentis*. Δ_{bio} was calculated from eq. 12 using the combined gas exchange and Δ measurements shown in Fig. 3. Δ_{bio} could not be calculated for *F. pringlei* because g_m is obtained from Δ measurements in this species, so both factors are not independent. Values represent averages and standard error of four replicates.

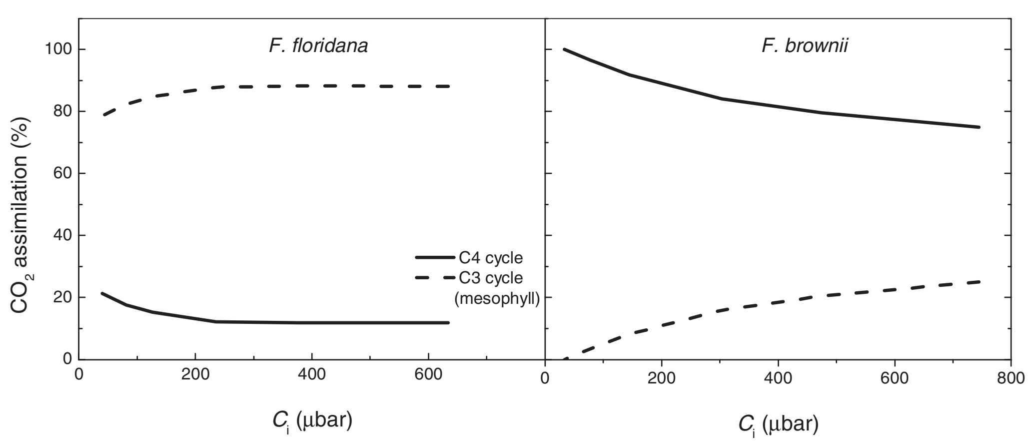

Fig. 8. CO_2 response of the estimated contribution of the C_4 cycle and the mesophyll C_3 cycle in the intermediate species *F. floridana* and *F. brownii*, expressed as a percent of total CO_2 assimilation rate, under low pO_2.

Downloaded from http://jxb.oxfordjournals.org/ at Australian National University on January 10, 2017

Discussion

Effect of O_2 on carbon assimilation and compensation point

The oxygen responses of CO_2 assimilation and the compensation point have been used in the past as a tool to identify and characterize C_3-C_4 intermediate species (Sayre and Kennedy, 1977; Monson *et al.*, 1984; Dai *et al.*, 1996; Vogan *et al.*, 2007). As only mesophyll Rubisco is exposed to air oxygen, its effect on CO_2 assimilation and Γ decreases with increasing proportions of the enzyme allocated to the bundle sheath. However, it is difficult to separate and quantify the effects of the C_2 and C_4 cycles from studies on the O_2 response of CO_2 assimilation, as both cycles contribute to reduce the negative effect of photorespiration in carbon assimilation and the compensation point. Moreover, the efficiency of the C_2 cycle varies between different intermediate species, as does the contribution of the C_4 cycle (Cheng *et al.*, 1988; Keerberg *et al.*, 2014).

In this work, the O_2 response of carbon assimilation, and especially Γ, in *F. brownii* was very close to that of the C_4 species *F. bidentis*. A highly efficient C_2 cycle would have a greater impact on the O_2 sensitivity of Γ than on carbon assimilation and that, combined with high *in vitro* PEPC and CA activities at the same level as the C_4 species *F. bidentis*, eliminates the effect of pO_2 on Γ almost completely (Cheng *et al.*, 1988; Ku *et al.*, 1991). Previous studies initially classified *F. brownii* as a C_4 species, but it was later demonstrated that the enzyme compartmentation is incomplete in this plant (Monson *et al.*, 1987; Ku *et al.*, 1991). The small proportion of Rubisco present in the mesophyll is reflected in the sensitivity of assimilation rate to pO_2.

CA activity in *F. floridana* is similar to *F. pringlei* but PEPC activity is four times higher (13.8 μmol m^{-2} s^{-1}), consistent with Ku *et al.* (1991) and supporting the hypothesis of an active C_4 cycle. However, PEPC activity is still low when compared with *F. bidentis* (91.8 μmol m^{-2} s^{-1}), indicating that the activity of the C_4 cycle in this plant is small. In our experiments, the O_2 sensitivity of Γ in *F. floridana* is intermediate, and the O_2 response of CO_2 assimilation rate is remarkably close to that of *F. brownii*.

Previous studies have reported a C_3-like O_2 response in *F. floridana* (Dai *et al.*, 1996; Monson *et al.*, 1986), which differs from our observations. Although the reason for this discrepancy is not known, it must be noted that O_2 sensitivity measurements are affected by variation of parameters like temperature or stomatal conductance between measurements at different pO_2. These interactions increase the difficulty of estimating the activity of the C_4 cycle from O_2 response experiments.

Signature of C_4 photosynthesis in the CO_2 response of Δ in intermediate species

The different CO_2 responses of *Δ* in the intermediate C_3-C_4 species, relative to the C_3 or C_4 species, can be attributed to the different ratios of PEPC/Rubisco activity in the mesophyll. The lower *Δ* observed in *F. floridana*, relative to *F. pringlei,* is partially attributable to a lower C_i/C_a, but their different Δ_{bio} indicates an influence of the PEPC to Rubisco ratio, especially at low C_i.

Interestingly, *F. brownii* and *F. bidentis* show similar *Δ* at low C_i, but it increases in *F. brownii* with increasing pCO_2 instead of decreasing as in the C_4 plant. This particular response can be attributed to the activity of the small fraction of Rubisco in the mesophyll that would have a stronger influence at high pCO_2. In *F. floridana*, Rubisco is abundant in the mesophyll but PEPC activity is low, and as a consequence the greatest effect of the C_4 cycle activity is observed at very low pCO_2, with a greater reduction of *Δ* compared to the C_3 species. Both results indicate that the contribution of mesophyll Rubisco to overall assimilation is more important under high pCO_2, and of the C_4 cycle at low pCO_2. The fact that environmental conditions affect the contribution of C_4 photosynthesis may explain ambiguous results on previous analyses of dry matter $\delta^{13}C$ in *F. floridana* and other intermediates, which showed C_3-like ratios (Monson *et al.*, 1988; Byrd *et al.*, 1992). $\delta^{13}C$ is a result of carbon discrimination during the leaf growth, thus it integrates the effect of variable environmental conditions. In the online experiments presented here, instant discrimination is measured under controlled conditions, highlighting their influence. By performing the analyses under low pO_2, the effect of photorespiration and subsequent refixation through the C_2 cycle is greatly reduced, emphasizing the differences in biochemical fractionation caused by the presence of C_4 activity.

Although the CO_2 response of *A* is also influenced by different relative activities of mesophyll Rubisco and PEPC, the effect of each enzyme in this case is difficult to separate. The greater initial slope of the A/C_i curve in *F. floridana*, compared with *F. pringlei*, reflects the slightly greater PEPC activity detected in our *in vitro* assays, but could also be attributed to higher Rubisco activity. In the same sense, the initial slope of the A/C_i curve in *F. brownii* and *F. bidentis* are similar and typically C_4, whereas their *Δ* are different.

Concurrent model fitting reveals C_4 activity in F. floridana

The strategy to evaluate the contribution of the C_4 cycle to total carbon assimilation in intermediate species presented in this work is based on concurrently measuring and model-fitting the CO_2 responses of carbon assimilation and discrimination.

Mathematical modeling has proved to be a powerful tool to get a deeper insight into the biochemical and physiological basis of the observed responses of carbon assimilation and discrimination, and it has been used to estimate parameters such as the maximum carboxylase activity of Rubisco *in vivo* ($V_{C,max}$) and g_m in C_3 species, or $V_{P,max}$ and leakiness in C_4 systems (Tazoe *et al.*, 2011; Ubierna *et al.*, 2011; Walker *et al.*, 2013; Sharwood and Whitney, 2014). However, in most cases there is more than one unknown variable in the equations that represent those responses. This is especially problematic in intermediate species, where the number of factors affecting those responses is greater than in C_3 or C_4

Downloaded from http://jxb.oxfordjournals.org/ at Australian National University on January 10, 2017

plants. By concurrently fitting the CO_2 responses of A and Δ in each experiment with the same set of constants, the range of values that can be assigned to these variables to obtain a satisfactory fitting is reduced. In this work, the activities of photosynthetic enzymes were analyzed *in vitro* to further reduce the number of unknowns, providing more accurate predictions. This method confirmed the presence of Rubisco activity in the mesophyll of *F. brownii*, which was already known (Cheng *et al.*, 1988), but more interestingly indicated that *F. floridana* harbors an active C_4 cycle. This C_4 activity causes a change in the biochemical fractionation, compared to *F. pringlei*, which is evident at any C_i analyzed. This is consistent with the increased activity of PEPC and previous observations based on $^{14}CO_2$ pulse-chase experiments (Monson *et al.*, 1986; von Caemmerer and Hubick, 1989). It is important to note that other studies based on $\delta^{13}C$ analyses, metabolite dynamics and O_2 response of carbon assimilation and Γ were unable to conclusively prove a contribution of the C_4 cycle to overall photosynthesis in *F. floridana*, and the presence of a futile C_4 cycle was proposed where most or all the CO_2 released in the bundle sheath is not fixed and leaks back to the mesophyll (Monson *et al.*, 1988; Leegood and von Caemmerer, 1994; Dai *et al.*, 1996). However, other authors have already indicated that in *F. floridana* the C_4 cycle may contribute up to 50% of the total CO_2 fixation (Ku *et al.*, 1991). In this work, the contribution of the mesophyll and the bundle sheath Rubisco to overall carbon assimilation was calculated for *F. brownii* and *F. floridana*. In both intermediate species, the contribution of the C_4 cycle, or bundle sheath Rubisco, is highest at very low pCO_2, and decreases with increasing pCO_2. This reflects the lower apparent K_c of PEPC compared to that of Rubisco (Bauwe, 1986; Kubien *et al.*, 2008).

An improved equation describing CO_2 response of Δ in intermediate species

An equation describing photosynthetic carbon isotope discrimination (Δ) that is applicable for C_3, C_4 and C_3-C_4 photosynthesis is provided and applied in this study. It allows the calculation of the biochemical fractionation occurring for the different photosynthetic pathways as a function of C_i and takes into account g_m and the ternary effects of transpiration rate. The biological relevance of g_m, and its influence on Δ, has been reported extensively and incorporated in mathematical models for C_3 species (Evans *et al.*, 1986; von Caemmerer and Evans, 1991; Tazoe *et al.*, 2011). When mesophyll conductance is considered in C_3 species, C_c (pCO_2 at the site of Rubisco) can be estimated and is lower than C_i, and this affects the estimates of Rubisco carboxylations. The same applies in intermediate species, where assimilation and discrimination by mesophyll Rubisco is dependent on the concentration of CO_2 diffusing from the intercellular space. For model fitting purposes, the calculated C_c was used as the available CO_2 for both PEPC and mesophyll Rubisco in the case of the intermediate species. The models presented in this work assume that pCO_2 is the same in the cytosol and the chloroplast.

The effect of pCO_2 on g_m has been studied by other authors, with results depending on the species analyzed. Whereas previous results showed that g_m is not affected by pCO_2 in wheat (Tazoe *et al.*, 2009), other authors reported an inverse correlation in several C_3 species (Flexas *et al.*, 2007; Tazoe *et al.*, 2011). We observed that g_m is dependent on pCO_2 in the C_3 *F. pringlei*, and assumed that the same is true for the C_4 and intermediate species analyzed. Although the effect of using either constant or variable g_m on the models of the CO_2 responses of carbon assimilation and discrimination has only a minor effect at low C_i, it is important for the calculation of Δ_{bio} and thus the contribution of the C_4 and C_3 cycles to overall carbon assimilation, especially at low C_i. The fact that Δ_{bio} is similar when calculated using either constant or variable g_m in *F. brownii* and *F. bidentis* reflects the lower relevance of g_m when the CO_2 concentrating mechanism is expressed at high levels.

Downloaded from http://jxb.oxfordjournals.org/ at Australian National University on January 10, 2017

Conclusion

Concurrent Δ and gas exchange measurements and modeling provide a powerful diagnostic tool for C_4 photosynthesis. Performing the measurements under controlled environmental conditions, especially low pO_2, allows the detection and estimation of the C_4 cycle activity in C_3-C_4 intermediate species even when it is low. This approach confirmed the presence of active Rubisco in the mesophyll of *F. brownii*, and revealed a contribution of the C_4 cycle to total carbon assimilation in *F. floridana*. However, the carbon isotope signal is complex and not all its components are well understood, so some caution is required. We show for example that a CO_2 dependence of g_m affects the calculation of the biochemical fractionation, and thus the contribution of the C_4 cycle to overall CO_2 assimilation.

Supplementary data

Supplementary data are available from *JXB* online.

Figure S1. Responses of C_i and stomatal conductance to changes in atmospheric pO_2.

Figure S2. Models of CO_2 response of assimilation rate and carbon isotope discrimination in the C_3 and C_4 species.

Figure S3. Effect of assuming constant or variable g_m in the calculation of the biochemical fractionation.

Acknowledgments

We thank Soumi Bala for expert technical assistance with plant culture, biochemical assays, TDL and gas exchange measurements. We thank the High Resolution Plant Phenomics Centre (CSIRO, Australia) for the use of their TDL for some experiments. This research was supported by the Bill and Melinda Gates Foundation's funding for the C_4 Rice consortium and by the Australian Research Council Centre of Excellence for Translational Photosynthesis (CE140100015).

References

Badger MR, Price GD. 1989. Carbonic anhydrase activity associated with the *Cyanobacterium Synechococcus* PCC7942. Plant Physiology **89,** 51–60.

Badger MR, Price GD. 1994. The role of carbonic anhydrase in photosynthesis. Annual Review of Plant Physiology and Plant Molecular Biology **45,** 369–392.

Bauwe H. 1986. An efficient method for the determination of K_m values for HCO^{3-} of phosphoenolpyruvate carboxylase. Planta **169,** 356–360.

Bowling DR, Sargent SD, Tanner BD, Ehleringer JR. 2003. Tunable diode laser absorption spectroscopy for stable isotope studies of ecosystem–atmosphere CO_2 exchange. Agricultural and Forest Meteorology **118,** 1–19.

Brown RH, Hattersley PW. 1989. Leaf anatomy of C_3-C_4 species as related to evolution of C_4 photosynthesis. Plant Physiology **91,** 1543–1550.

Brown WV. 1975. Variations in anatomy, associations, and origins of Kranz tissue. American Journal of Botany **11,** 395–402.

Byrd GT, Brown RH. 1989. Environmental effects on photorespiration of C_3-C_4 species: I. Influence of CO_2 and O_2 during growth on photorespiratory characteristics and leaf anatomy. Plant Physiology **90,** 1022–1028.

Byrd GT, Brown RH, Bouton JH, Bassett CL, Black CC. 1992. Degree of C_4 photosynthesis in C_4 and C_3-C_4 *Flaveria* species and their hybrids: I. CO_2 assimilation and metabolism and activities of phosphoenolpyruvate carboxylase and NADP-malic enzyme. Plant Physiology **100,** 939–946.

Cheng S-H, Moore BD, Edwards GE, Ku MSB. 1988. Photosynthesis in *Flaveria brownii*, a C_4-like species: leaf anatomy, characteristics of CO_2 exchange, compartmentation of photosynthetic enzymes, and metabolism of $^{14}CO_2$. Plant Physiology **87,** 867–873.

Cousins AB, Badger MR, von Caemmerer S. 2008. C_4 photosynthetic isotope exchange in NAD-ME- and NADP-ME-type grasses. Journal of Experimental Botany **59,** 1695–1703.

Dai Z, Ku MB, Edwards G. 1996. Oxygen sensitivity of photosynthesis and photorespiration in different photosynthetic types in the genus *Flaveria*. Planta **198,** 563–571.

Ehleringer JR, Sage RF, Flanagan LB, Pearcy RW. 1991. Climate change and the evolution of C_4 photosynthesis. Trends in Ecology & Evolution **6,** 95–99.

Evans JR, Sharkey TD, Berry JA, Farquhar GD. 1986. Carbon isotope discrimination measured concurrently with gas exchange to investigate CO_2 diffusion in leaves of higher plants. Functional Plant Biology **13,** 281–292.

Evans JR, von Caemmerer S, Setchell BA, Hudson GS. 1994. the relationship between CO_2 transfer conductance and leaf anatomy in transgenic tobacco with a reduced content of Rubisco. Functional Plant Biology **21,** 475–495.

Evans JR, von Caemmerer S. 2013. Temperature response of carbon isotope discrimination and mesophyll conductance in tobacco. Plant, Cell & Environment **36,** 745–756.

Farquhar GD. 1983. On the Nature of carbon isotope discrimination in C_4 species. Functional Plant Biology **10,** 205–226.

Farquhar GD, O'Leary MH, Berry J. 1982. On the relationship between carbon isotope discrimination and the intercellular carbon dioxide concentration in leaves. Functional Plant Biology **9,** 121–137.

Farquhar GD, Cernusak LA. 2012. Ternary effects on the gas exchange of isotopologues of carbon dioxide. Plant, Cell & Environment **35,** 1221–1231.

Flexas J, Diaz-Espejo A, Galmés J, Kaldenhoff R, Medrano H, Ribas-Carbo M. 2007. Rapid variations of mesophyll conductance in response to changes in CO_2 concentration around leaves. Plant, Cell & Environment **30,** 1284–1298.

Griffis TJ, Baker JM, Sargent SD, Tanner BD, Zhang J. 2004. Measuring field-scale isotopic CO_2 fluxes with tunable diode laser absorption spectroscopy and micrometeorological techniques. Agricultural and Forest Meteorology **124,** 15–29.

Griffiths H, Cousins AB, Badger MR, von Caemmerer S. 2007. Discrimination in the dark. Resolving the interplay between metabolic and physical constraints to phosphoenolpyruvate carboxylase activity during the crassulacean acid metabolism cycle. Plant Physiology **143,** 1055–1067.

Hatch MD. 1987. C_4 photosynthesis – a unique blend of modified biochemistry, anatomy and ultraestructure. Biochimica et Biophysica Acta **895,** 81–106.

Hatch MD, Slack CR, Johnson HS. 1967. Further studies on a new pathway of photosynthetic carbon dioxide fixation in sugar-cane and its occurrence in other plant species. The Biochemical Journal **102,** 417–422.

Henderson SA, von Caemmerer S, Farquhar GD. 1992. Short-term measurements of carbon isotope discrimination in several C_4 species. Functional Plant Biology **19,** 263–285.

Hibberd JM, Sheehy JE, Langdale JA. 2008. Using C_4 photosynthesis to increase the yield of rice-rationale and feasibility. Current Opinion in Plant Biology **11,** 228–231.

Holaday AS, Lee K, Chollet R. 1984. C_3–C_4 Intermediate species in the genus *Flaveria*: leaf anatomy, ultrastructure, and the effect of O_2 on the CO_2 compensation concentration. Planta **160,** 25–32.

Jenkins CL, Furbank RT, Hatch MD. 1989. Mechanism of C_4 photosynthesis: a model describing the inorganic carbon pool in bundle sheath cells. Plant Physiology **91,** 1372–1381.

Karki S, Rizal G, Quick W. 2013. Improvement of photosynthesis in rice (*Oryza sativa* L.) by inserting the C_4 pathway. Rice **6,** 28.

Keerberg O, Pärnik T, Ivanova H, Bassüner B, Bauwe H. 2014. C_2 photosynthesis generates about 3-fold elevated leaf CO_2 levels in the C_3–C_4 intermediate species *Flaveria pubescens*. Journal of Experimental Botany **65,** 3649–3656.

Ku MS, Monson RK, Littlejohn RO, Nakamoto H, Fisher DB, Edwards GE. 1983. Photosynthetic characteristics of C_3-C_4 intermediate *flaveria* species: i. leaf anatomy, photosynthetic responses to O_2 and CO_2, and activities of key enzymes in the C_3 and C_4 pathways. Plant Physiology **71,** 944–948.

Ku MSB, Wu J, Dai Z, Scott RA, Chu C, Edwards GE. 1991. Photosynthetic and photorespiratory characteristics of *Flaveria* species. Plant Physiology **96,** 518–528.

Kubien DS, Whitney SM, Moore PV, Jesson LK. 2008. The biochemistry of Rubisco in *Flaveria*. Journal of Experimental Botany **59,** 1767–1777.

Langdale JA. 2011. C_4 cycles: past, present, and future research on C_4 photosynthesis. The Plant Cell **23,** 3879–3892.

Leegood RC. 2013. Strategies for engineering C_4 photosynthesis. Journal of Plant Physiology **170,** 378–388.

Leegood RC, von Caemmerer S. 1994. Regulation of photosynthetic carbon assimilation in leaves of C_3–C_4 intermediate species of *Moricandia* and *Flaveria*. Planta **192,** 232–238.

McKown AD, Moncalvo JM, Dengler NG. 2005. Phylogeny of *Flaveria* (Asteraceae) and inference of C_4 photosynthesis evolution. American Journal of Botany **92,** 1911–1928.

Monson RK, Edwards GE, Ku MSB. 1984. C_3-C_4 intermediate photosynthesis in plants. BioScience **34,** 563–574.

Monson RK, Moore Bd, Ku MSB, Edwards GE. 1986. Co-function of C_3-and C_4-photosynthetic pathways in C_3, C_4 and C_3-C_4 intermediate *Flaveria* species. Planta **168,** 493–502.

Monson RK, Schuster WS, Ku MSB. 1987. Photosynthesis in *Flaveria brownii* AM Powell: a C_4-Like C_3-C_4 intermediate. Plant physiology **85,** 1063–1067.

Monson RK, Teeri JA, Ku MSB, Gurevitch J, Mets LJ, Dudley S. 1988. Carbon-isotope discrimination by leaves of *Flaveria* species exhibiting different amounts of C_3-and C_4-cycle co-function. Planta **174,** 145–151.

Moore BD, Ku MSB, Edwards GE. 1989. Expression of C_4-like photosynthesis in several species of *Flaveria*. Plant, Cell & Environment **12,** 541–549.

O'Leary MH. 1981. Carbon isotope fractionation in plants. Phytochemistry **20,** 553–567.

Pengelly JJ, Tan J, Furbank RT, von Caemmerer S. 2012. Antisense reduction of NADP-malic enzyme in *Flaveria bidentis* reduces flow of CO_2 through the C_4 cycle. Plant Physiology **160,** 1070–1080.

Pengelly JJL, Sirault XRR, Tazoe Y, Evans JR, Furbank RT, von Caemmerer S. 2010. Growth of the C_4 dicot *Flaveria bidentis*: photosynthetic acclimation to low light through shifts in leaf anatomy and biochemistry. Journal of Experimental Botany **61,** 4109–4122.

Rawsthorne S. 1992. C_3–C_4 intermediate photosynthesis: linking physiology to gene expression. The Plant Journal **2,** 267–274.

Roeske CA, O'Leary MH. 1984. Carbon isotope effects on enzyme-catalyzed carboxylation of ribulose bisphosphate. Biochemistry **23,** 6275–6284.

Sage RF, Christin PA, Edwards EJ. 2011. The C_4 plant lineages of planet Earth. Journal of Experimental Botany **62,** 3155–3169.

Downloaded from http://jxb.oxfordjournals.org/ at Australian National University on January 10, 2017

Sage RF, Sage TL, Kocacinar F. 2012. Photorespiration and the evolution of C_4 photosynthesis. Annual Review of Plant Biology **63,** 19–47.

Sayre RT, Kennedy RA. 1977. Ecotypic differences in the C_3 and C_4 photosynthetic activity in *Mollugo verticillata*, a C_3–C_4 intermediate. Planta **134,** 257–262.

Schulze S, Mallmann J, Burscheidt J, Koczor M, Streubel M, Bauwe H, Gowik U, Westhoff P. 2013. Evolution of C_4 photosynthesis in the genus *Flaveria*: establishment of a photorespiratory CO_2 pump. The Plant Cell **25,** 2522–2535.

Sharwood RE, Whitney SM. 2014. Correlating Rubisco catalytic and sequence diversity within C_3 plants with changes in atmospheric CO_2 concentrations. Plant, Cell & Environment **37,** 1981–1984.

Tazoe Y, von Caemmerer S, Badger MR, Evans JR. 2009. Light and CO_2 do not affect the mesophyll conductance to CO_2 diffusion in wheat leaves. Journal of Experimental Botany **60,** 2291–2301.

Tazoe Y, von Caemmerer S, Estavillo GM, Evans JR. 2011. Using tunable diode laser spectroscopy to measure carbon isotope discrimination and mesophyll conductance to CO_2 diffusion dynamically at different CO_2 concentrations. Plant, Cell & Environment **34,** 580–591.

Tholen D, Zhu XG. 2011. The mechanistic basis of internal conductance: a theoretical analysis of mesophyll cell photosynthesis and CO_2 diffusion. Plant Physiology **156,** 90–105.

Ubierna N, Sun W, Cousins AB. 2011. The efficiency of C_4 photosynthesis under low light conditions: assumptions and calculations with CO_2 isotope discrimination. Journal of Experimental Botany **62,** 3119–3134.

Vogan PJ, Frohlich MW, Sage RF. 2007. The functional significance of C_3–C_4 intermediate traits in *Heliotropium* L. (Boraginaceae): gas exchange perspectives. Plant, Cell & Environment **30,** 1337–1345.

von Caemmerer S. 1992. Carbon isotope discrimination in C_3-C_4 intermediates. Plant, Cell & Environment **15,** 1063–1072.

von Caemmerer S. 2000. Biochemical Models of Leaf Photosynthesis . Vol. **2**. CSIRO Publishing, Collingwood, Australia.

von Caemmerer S. 2013. Steady-state models of photosynthesis. Plant, Cell & Environment **36,** 1617–1630.

von Caemmerer S, Evans JR. 1991. Determination of the average partial pressure of CO_2 in chloroplast from leaves of several C_3 plants. Australian Journal of Plant Physiology **18,** 287–305.

von Caemmerer S, Ghannoum O, Pengelly JJL, Cousins AB. 2014. Carbon isotope discrimination as a tool to explore C_4 photosynthesis. Journal of Experimental Botany **65,** 3459–3470.

von Caemmerer S, Hubick KT. 1989. Short-term carbon-isotope discrimination in C_3–C_4 intermediate species. Planta **178,** 475–481.

von Caemmerer S, Quick WP. 2000. Rubisco: physiology in vivo. In: Leegood R, Sharkey T, von Caemmerer S, eds. Photosynthesis , Vol. **9**: Springer Netherlands, 85–113.

von Caemmerer S, Quick WP, Furbank RT. 2012. The development of C_4 rice: current progress and future challenges. Science **336,** 1671–1672.

von Caemmerer S, Quinn V, Hancock NC, Price GD, Furbank RT, Ludwig M. 2004. Carbonic anhydrase and C_4 photosynthesis: a transgenic analysis. Plant, Cell & Environment **27,** 697–703.

Walker B, Ariza LS, Kaines S, Badger MR, Cousins AB. 2013. Temperature response of in vivo Rubisco kinetics and mesophyll conductance in *Arabidopsis thaliana*: comparisons to Nicotiana tabacum. Plant, Cell & Environment **36,** 2108–2119.

Wang L, Czedik-Eysenberg A, Mertz RA, et al. 2014. Comparative analyses of C4 and C3 photosynthesis in developing leaves of maize and rice. Nature Biotechnology **32,** 1158–1165.

Whitney SM, Sharwood RE, Orr D, White SJ, Alonso H, Galmés J. 2011. Isoleucine 309 acts as a C_4 catalytic switch that increases ribulose-1,5-bisphosphate carboxylase/oxygenase (rubisco) carboxylation rate in *Flaveria*. Proceedings of the National Academy of Sciences, USA **108,** 14688–14693.

Wingate L, Seibt U, Moncrieff JB, Jarvis PG, Lloyd JON. 2007. Variations in ^{13}C discrimination during CO_2 exchange by *Picea sitchensis* branches in the field. Plant, Cell & Environment **30,** 600–616.

Downloaded from http://jxb.oxfordjournals.org/ at Australian National University on January 10, 2017